




# A High-Gain Hemispherical Dielectric Lens Antenna Operating Simultaneously in Narrowband or Wideband for X-band Applications

R. A. dos Santos<sup>1</sup> , G. L. S. Fré<sup>2</sup> , D. H. Spadoti<sup>3</sup> 

<sup>1</sup>Faculty of Electrical Engineering, Federal University of Uberlândia - UFU, Minas Gerais, Brazil, [renans@ufu.br](mailto:renans@ufu.br)

<sup>2</sup>FIT Tecnologia, Sorocaba, São Paulo, Brazil, [gabriel.fre@fit-tecnologia.org.br](mailto:gabriel.fre@fit-tecnologia.org.br)

<sup>3</sup>Telecommunication's Lab (LabTel), Federal University of Itajubá – UNIFEI, Minas Gerais, Brazil, [spadoti@unifei.edu.br](mailto:spadoti@unifei.edu.br)

**Abstract**— A hemispherical dielectric lens antenna is proposed to provide beam-steering for communication networks operating in X-band. Two different printed antennas are simultaneously used to guarantee high performance and diversity of applications, one a wideband linear polarized antenna, and the other a narrowband circular polarized antenna. To ensure this, the design relies on adding printed angled feeders correctly positioned in relation to the center of a homogeneous dielectric lens. A prototype was simulated, fabricated and tested. The measured results show that the antenna is capable of operating from 8.0 GHz to 12 GHz (gain of 14.2 dBi) or 9.5 GHz to 10 GHz (gain of 17.52 dBi).

**Index Terms**— Dielectric lens antenna, circularly-polarized, high gain, ultra-wideband lens antennas.

## I. INTRODUCTION

Multifunctional antennas have proven to be important for the future of telecommunications systems [1]-[3]. Antennas with more than one radiation and/or impedance characteristic are essential for cooperative use of different technologies in the same network infrastructure. Among the features stand out high gain [4]-[6], wideband [7]-[9] and circularly polarized [10]-[12].

X-band (8.0 GHz to 12 GHz) applications such as marine radars [13], CubeSat satellites [14] and radar systems [15] have driven the development of multifunctional antennas. In this way, lens antennas are promising solutions to overcome this challenge, due to design flexibility, low cost, polarization insensitivity and large bandwidth. In [16], a gradient index lens with a metalized thin-walled conical horn antenna, and a WR90 rectangular to linear polarized circular waveguide transition was simulated, fabricated, and measured. The lens antenna bandwidth was from 8.2 GHz to 12.4 GHz with an input reflection less than  $-15$  dB and peak gain of 18.7 dBi. In [17], a broadband 3-D-printed circularly polarized spherical Luneburg lens with the linearly polarized feed antenna for the X-band is simulated, fabricated, and measured. The lens antenna has a measured operational bandwidth of 8.0GHz to 12.0GHz with an input VSWR less than 2 and peak gain of 18.6dBi.

In this paper, a hemispherical dielectric lens design is simultaneously fed by two different antennas,

one a wideband design with linear polarization, and another a narrow band design with double polarization, guaranteeing high performance and diverse applications in X-band.

## II. FEEDERS DESIGN

The proposed geometry for the feeders of the dielectric lens antennas is detailed in Fig. 1(a). One is a broadband printed antenna (BPA) (see Fig. 1(a)) fed with a microstrip line, and designed with two modifications [18], [19]: a ground plane reduction, and a rounding of the lower vertices of the patch. The other is a circularly-polarized squared microstrip antenna (DPMA) (see Fig. 1(a)) fed with an offset coaxial probe [20]. The feeders were designed using the Arlon Diclac 880 dielectric substrate (with a relative permittivity of 2.17, a loss tangent of 0.0009 and an  $h = 1.52$  mm thickness). The design parameters were optimized using the finite elements method in ANSYS HFSS, and listed in Table I.

Fig. 2 shows the characteristics of the two feeders of the dielectric lens antenna. The results of the simulated reflection coefficient and the radiation pattern in  $yz$ -plane for both antennas are compared and presented in Figs. 2(a) and (b), respectively. The bandwidth ( $S_{11} \leq -10$  dB) covers a range of 8.0 to 12 GHz (for BPA) and 9.5 to 10 GHz (for DPMA). The ground plane reduction and rounding of the lower vertices of the patch are responsible for increasing the bandwidth of BPA to over 40% of the central frequency (10 GHz). The DPMA has a bandwidth similar to the conventional microstrip antenna (5.12%) due to the offset-feed. Therefore, these two feeders can work in wideband or narrowband, depending on the application, as shown, from  $S_{11}$  in Fig. 2(a). Radiation patterns in co-polarization (Co-Pol) and cross-polarization (X-Pol) are analyzed (shown in Fig. 2(b)). Due to the reduction of the ground plane, the BPA radiation pattern is almost omnidirectional. The radiation pattern varies between  $-2.5$  dBi and  $3.0$  dBi in the  $yz$ -plane (10 GHz). Moreover, due to the BPA feed (linear polarization) high polarization rejection occurs. The DPMA presents a similar radiation pattern to conventional microstrip antennas, i.e. with well-defined main lobe and low side-lobe levels. However, due to offset-feed, a maximum gain of  $3.0$  dBi (about  $3.0$  dB lower than conventional microstrip antennas due to the energy division in the two polarizations) was observed (9.75 GHz). In addition, a high similarity in the radiation patterns in Co-Pol and X-Pol was observed.

TABLE I. BPA AND DPMA DIMENSIONS (UNIT: MM)

BPA					DPMA			
$W$	$L$	$w_\ell$	$L_\ell$	$\rho$	$W$	$L$	$x_0$	$y_0$
12.9	9.60	4.87	3.20	3.87	9.60	9.60	3.48	3.48

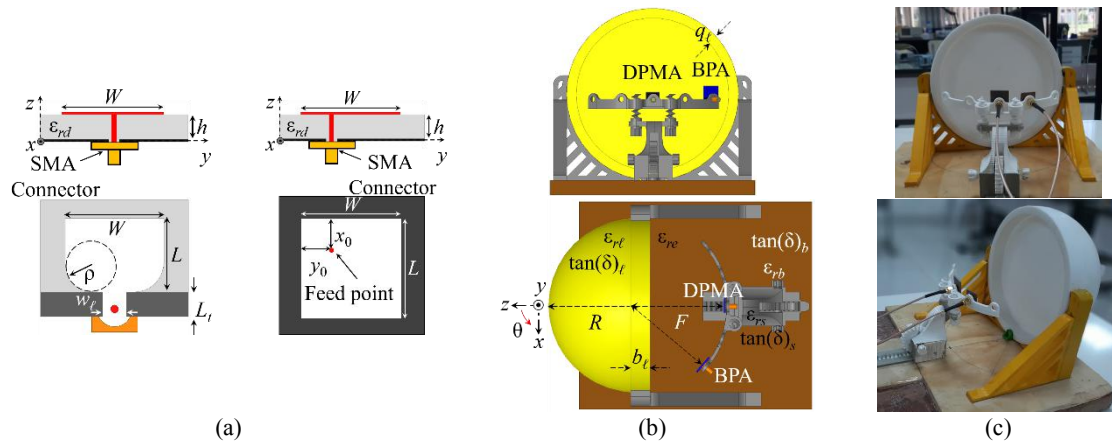


Fig. 1. Proposed antenna. (a) Feeders of the dielectric lens antennas. (b) Numerical model dielectric lens antennas. (c) Prototype dielectric lens antennas.

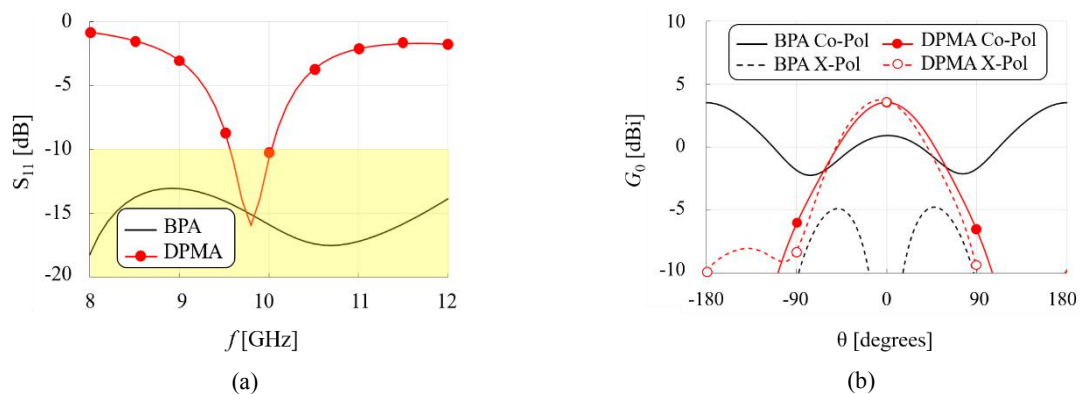


Fig. 2. Feeder characteristics. (a) Reflection coefficient. (b) Radiation pattern in  $yz$ -plane.

### III. DIELECTRIC LENS ANTENNAS DESIGN

The two feeders (BPA and DPMA) were coupled with a homogeneous hemispherical dielectric lens, as described in Fig. 1. The dielectric lens was made of polytetrafluoroethylene (PTFE), with relative permittivity ( $\epsilon_{rl}$ ) equal to 2.2, and loss tangent ( $\tan(\delta)_l$ ) equal 0.00015. The lens radius ( $R$ ) (see Fig. 1) is equal to  $3\lambda_0$  at 10 GHz ( $R = 90$  mm), in which  $\lambda_0$  is the free space wavelength.

The lens works as an energy collimator, producing high directivity, if the distance between the feeder and the flat lens surface (focal length,  $F$ ) is correctly sized. By considering air as the external medium ( $\epsilon_{re} = 1$ ) a value  $F = 96.2$  mm was found [21]. After determining the  $F$  value, the DPMA was positioned towards the center of the lens (perpendicularly) and the BPA positioned  $20^\circ$  from center (see Fig. 1).

A structure for fixing the lens was developed (see Fig. 1(b)-(c)). The structure consists of: a wood base (brown) with relative dielectric permittivity,  $\epsilon_{rb} = 1.22$ , and a dissipation factor,  $\tan(\delta)_b = 0.1$  [22]. The fixing structures were made from PLA (gray), with  $\epsilon_{rs} = 3.5$  and  $\tan(\delta)_s = 0.07$  [22]. In addition, a hollow cylindrical extension of PTFE was created in the lens (see Fig. 1(b)), with  $b_l = 20$  mm and  $q_l = 10$  mm, to facilitated fixing. Given the specifications, a prototype was constructed (see Fig. 1(c)), and measured.

### A. S-parameters

The simulated and measured S-parameters curves of the proposed dielectric lens antenna show a strong similarity, as presented in Fig 3. The difference between the curves is credited mainly to manufacturing errors or fluctuations in the material properties. The impedance bandwidth measured for  $S_{11} \leq -10$  dB covers 8.0 to 12 GHz for BPA, and 9.5 to 10 GHz for DPMA, without coupling between feeders (with  $S_{21} = S_{12} > -18$ dB).

### B. Radiation Performance

The measured and simulated radiation pattern of the proposed lens antenna were compared and presented in Fig. 4(a)-(d). The radiation pattern in Co-Pol was investigated in a range from 8.0 GHz to 10 GHz for the lens fed by the BPA. For the DPMA as a feeder, both Co-Pol and X-Pol were investigated at 9.75 GHz. It is important to highlight that in the radiation pattern and gain measurements of one feeder, the other was terminated with a matched load. The measured and simulated curves are extremely similar, proving the effectiveness of the proposed design. The gain values found for the two feeders are in line with the expected in theory [21].

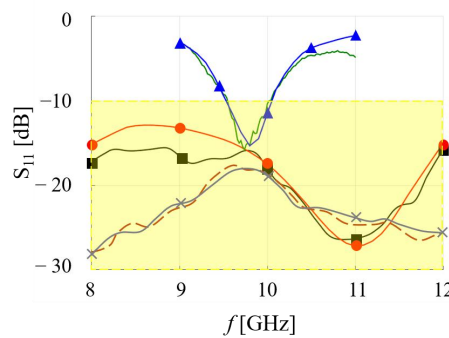


Fig. 3. The proposed lens antenna measured and simulated S-parameters. Blue curve with triangle (simulated) and green curve (measured) for reflection coefficient DPMA. Red curve with circles (simulated) and black curve with square (measured) for reflection coefficient BPA. Grey curve with X (simulated) and brown dotted curve for feeders coupling.

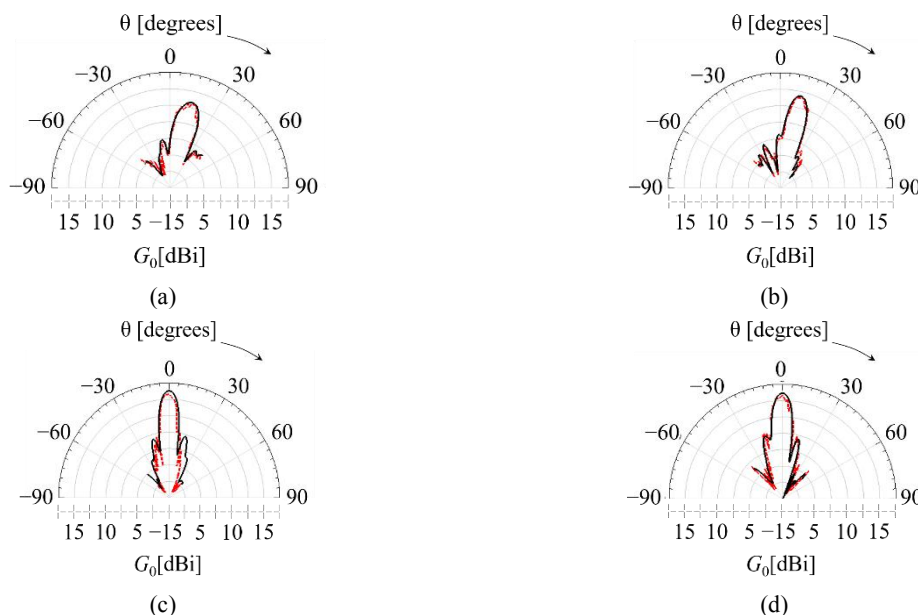


Fig. 4. The proposed lens antenna measured (red dotted curve) and simulated (black continuous curve) radiation pattern in the  $xz$ -plane. (a) BPA feeder in 8.0 GHz. (b) BPA feeder in 10 GHz. (c) DPMA feeder in Co-Pol and 9.75 GHz. (d) DPMA feeder in X-Pol and 9.75 GHz.

### C. Comparative study

A comparative study is presented in Table II of the proposed antenna with other designs of dielectric lens antennas. The number of applications that can respond simultaneously, the lens radius, the gain and the percentage bandwidth, were all compared. The Flat Lens Antennas [23] were designed with a radius of  $5\lambda_0$ , fed by an array of printed antennas, with gain of 18.00 dBi and a bandwidth of 14.00%. The Lens Antenna with Planar Focal Surface [24] was designed with a radius of  $3.1\lambda_0$ , fed by an array of printed antennas, with a gain of 16.65 dBi and a bandwidth of 5.94%. The Fresnel Multi-Zone Plate Lens Antenna [25] was designed with a radius of  $6.6\lambda_0$ , fed by an  $TE_{101}$  cavity device, with gain of 33.30 dBi and a bandwidth of 38.20%. The 3-D printed multibeam spherical lens antenna with 2-D ultrawide-angle coverage [26] was designed with a radius of  $1.4\lambda_0$ , fed by a compact CP patch antenna operating at X-band, with gain of 15.30 dBi and a bandwidth of 6.30%. The wideband high-gain double-sided dielectric lens integrated with a dual-bowtie Antenna [27] was designed with a radius of  $1.7\lambda_0$ , fed by a dual-bowtie antenna, with gain of 15.10 dBi and a bandwidth of 65.50%. The design of broadband 3-D-printed circularly polarized spherical luneburg lens antenna for X-band [28] was designed with a radius of  $3.00\lambda_0$ , fed by a vivaldi antenna, with gain of 18.60 dBi and a bandwidth of 40.00%. The compact high-gain wideband lens vivaldi antenna [29] was designed with a radius of  $1.80\lambda_0$ , fed by a Vivaldi antenna, with gain of 15.90 dBi and a bandwidth of 160.90%. In this study, we have proposed a hemispherical dielectric lens antenna that was designed with a radius of  $3\lambda_0$ . The simulated and measured results validate the functionality of the structure, capable of operating from 8.0 to 12 GHz (gain of 14.2 dBi) or 9.5 to 10 GHz (gain of 17.52 dBi), respectively, for BPA and DPMA antennas. The main innovation is the ability to meet the demand for more than one service with only one antenna. It is the first time that an antenna with these characteristics has been presented.

TABLE II. COMPARISON WITH PREVIOUS LITERATURE STUDIES OF DIELECTRIC LENS ANTENNAS.

Reference	Type feeders	Lens radius [ $\lambda_0$ ]	$G_0$ [dBi]	$Bw$ (%)
[23]	One application	5.0	18.00	14.00
[24]	One application	3.1	16.65	5.94
[25]	One application	6.6	33.30	38.20
[26]	One application	1.4	15.30	6.30
[27]	One application	1.7	15.10	65.5
[28]	One application	3.0	18.60	40.00
[29]	One application	1.8	15.90	160.9
This work	Two applications	3.0	14.20 <sup>a</sup>	40.00 <sup>a</sup>
			17.52 <sup>b</sup>	5.12 <sup>b</sup>

<sup>a</sup>Broadband printed antenna as feeder.

<sup>b</sup>Circularly-Polarized microstrip antenna as feeder.



#### IV. CONCLUSIONS

In this paper, a hemispheric dielectric lens antenna design was proposed for providing beam-steering in X-band networks. The lens was fed simultaneously by two printed antennas (one wideband antenna with linear polarization and the other narrowband antenna with circular polarization). The proposed antenna was designed, manufactured, and measured. The simulated and measured results show that the apparatus has the ability to cover the entire X-Band, operating from 8.0 GHz to 12 GHz with gain equal to 14.2 dBi, or operating from 9.5 GHz to 10 GHz with gain equal to 17.52 dBi. Thus, the proposed antenna may prove to be a promising innovation for the future of telecommunications systems.

#### ACKNOWLEDGMENT

The authors would like to acknowledge: UNIFEI's LabTel and LAIoI Group, CAPES, CNPQ, FAPEMIG, Intel Competence Center, and the National Institute of Telecommunications – INATEL, Brazil.

#### REFERENCES

- [1] Z. Wang, S. Liu and Y. Dong, "Low-Profile Multifunctional Pattern Reconfigurable Antenna Using Periodic Capacitor-Loaded Surface for 5G and Beyond," in *IEEE Transactions on Antennas and Propagation*, vol. 70, no. 5, pp. 3277-3286, May 2022.
- [2] S. Yang, Z. Yan, T. Zhang, M. Cai, F. Fan and X. Li, "Multifunctional Tri-Band Dual-Polarized Antenna Combining Transmitarray and Reflectarray," in *IEEE Transactions on Antennas and Propagation*, vol. 69, no. 9, pp. 6016-6021, Sept. 2021.
- [3] G. Mishra and S. K. Sharma, "A Multifunctional Full-Polarization Reconfigurable 28 GHz Staggered Butterfly 1-D-Beam Steering Antenna," in *IEEE Transactions on Antennas and Propagation*, vol. 69, no. 10, pp. 6468-6479, Oct. 2021.
- [4] E. Baldazzi et al., "A High-Gain Dielectric Resonator Antenna With Plastic-Based Conical Horn for Millimeter-Wave Applications," in *IEEE Antennas and Wireless Propagation Letters*, vol. 19, no. 6, pp. 949-953, June 2020.
- [5] L. Leszkowska, M. Rzymowski, K. Nyka and L. Kulas, "High-Gain Compact Circularly Polarized X-Band Superstrate Antenna for CubeSat Applications," in *IEEE Antennas and Wireless Propagation Letters*, vol. 20, no. 11, pp. 2090-2094, Nov. 2021.
- [6] Y. Chen et al., "Landstorfer Printed Log-Periodic Dipole Array Antenna With Enhanced Stable High Gain for 5G Communication," in *IEEE Transactions on Antennas and Propagation*, vol. 69, no. 12, pp. 8407-8414, Dec. 2021.
- [7] L. -H. Wen et al., "A Wideband Series-Fed Circularly Polarized Differential Antenna by Using Crossed Open Slot-Pairs," in *IEEE Transactions on Antennas and Propagation*, vol. 68, no. 4, pp. 2565-2574, April 2020.
- [8] R. Cicchetti, V. Cicchetti, A. Faraone, L. Foged and O. Testa, "A Compact High-Gain Wideband Lens Vivaldi Antenna for Wireless Communications and Through-the-Wall Imaging," in *IEEE Transactions on Antennas and Propagation*, vol. 69, no. 6, pp. 3177-3192, June 2021.
- [9] Z. Chen et al., "Compact Wideband Circularly Polarized Loop Antenna Based on Dual Common and Differential Modes," in *IEEE Antennas and Wireless Propagation Letters*, vol. 21, no. 8, pp. 1567-1571, Aug. 2022.
- [10] S. -S. Hao, Q. -Q. Chen, J. -Y. Li and J. Xie, "A High-Gain Circularly Polarized Slotted Patch Antenna," in *IEEE Antennas and Wireless Propagation Letters*, vol. 19, no. 6, pp. 1022-1026, June 2020.
- [11] Y. Liu et al., "A K-Band Broadband Circularly Polarized Slot Antenna Based on L-Shaped Waveguide Cavity," in *IEEE Antennas and Wireless Propagation Letters*, vol. 20, no. 9, pp. 1606-1610, Sept. 2021.
- [12] Y. Cheng and Y. Dong, "Wideband Circularly Polarized Split Patch Antenna Loaded With Suspended Rods," in *IEEE Antennas and Wireless Propagation Letters*, vol. 20, no. 2, pp. 229-233, Feb. 2021.
- [13] R. Banerjee, S. K. Sharma, J. -C. S. Chieh and R. Farkouh, "Investigations of Heat Sink Property of a Novel Dual Linear Polarized Low Cross-Polarization X-Band Phased Array Antenna Employing Silicon RFICs-Based Beamforming Network," in *IEEE Open Journal of Antennas and Propagation*, vol. 3, pp. 523-537, 2022.
- [14] L. Leszkowska, M. Rzymowski, K. Nyka and L. Kulas, "High-Gain Compact Circularly Polarized X-Band Superstrate Antenna for CubeSat Applications," in *IEEE Antennas and Wireless Propagation Letters*, vol. 20, no. 11, pp. 2090-2094, Nov. 2021.
- [15] N. Aboserwal, J. L. Salazar-Cerreno and Z. Qamar, "An Ultra-Compact X-Band Dual-Polarized Slotted Waveguide Array Unit Cell for Large E-Scanning Radar Systems," in *IEEE Access*, vol. 8, pp. 210651-210662, 2020.
- [16] I. Goode and C. E. Saavedra, "3D Printed Linearly Polarized X-Band Conical Horn Antenna and Lens," in *IEEE Open Journal of Antennas and Propagation*, vol. 3, pp. 549-556, 2022.

- [17] S. Lei, K. Han, X. Li and G. Wei, "A Design of Broadband 3-D-Printed Circularly Polarized Spherical Luneburg Lens Antenna for X-Band," in *IEEE Antennas and Wireless Propagation Letters*, vol. 20, no. 4, pp. 528-532, April 2021.
- [18] R. dos Santos, A. M. Muniz, M. Borsato, T. H. Brandão, T. N. Rodovalho and S. A. Cerqueira, "Multi-technology wireless coverage based on a leaky-wave reconfigurable antenna," in *2017 11th European Conference on Antennas and Propagation (EUCAP)*, pp. 2824-2828, Paris, 2017.
- [19] G. Pandey, P. J. Soh1,3, M. Mercuri, A. Beyer, G. A. E. Vandenbosch, and D. Schreurs, "EM-based Antenna Optimization for Health Monitoring Radar Sensor," in *29<sup>th</sup> Annual Review of Progress in Applied Computational Electromagnetics*, Monterey, 2013.
- [20] D. C. Nascimento, B. M. Fabiani, and J. C. S. Lacava, "Performance Analysis of Probe-Fed Circularly-Polarized Moderately-Thick Microstrip Antennas Designed under the Null Reactance Condition," *Journal of Microwaves, Optoelectronics and Electromagnetic Applications*, Vol. 17, No. 1 March 2018.
- [21] R. A. dos Santos, G. L. Fré and D. H. Spadoti, "Technique for constructing hemispherical dielectric lens antennas," in *Microwave and Optical Technology Letters*, 2019.
- [22] P. A. Rizzi, "Microwave Engineering: Passive Circuits", 1st Edition, Prentice-Hall, 1988.
- [23] M. Imbert, J. Romeu, M. Baquero-Escudero, M. Martinez-Ingles, J. Molina-Garcia-Pardo and L. Jofre, "Assessment of LTCC-Based Dielectric Flat Lens Antennas and Switched-Beam Arrays for Future 5G Millimeter-Wave Communication Systems," in *IEEE Transactions on Antennas and Propagation*, vol. 65, no. 12, pp. 6453-6473, Dec. 2017.
- [24] J. G. Marin and J. Hesselbarth, "Lens Antenna with Planar Focal Surface for Wide-Angle Beam-Steering Application," in *IEEE Transactions on Antennas and Propagation*, Early Access, January 2019.
- [25] J. M. Monkevich and G. P. Le Sage, "Design and Fabrication of a Custom-Dielectric Fresnel Multi-Zone Plate Lens Antenna Using Additive Manufacturing Techniques," in *IEEE Access*, vol. 7, pp. 61452-61460, 2019.
- [26] K. Liu, C. Zhao, S. -W. Qu, Y. Chen, J. Hu and S. Yang, "A 3-D-Printed Multibeam Spherical Lens Antenna With Ultrawide-Angle Coverage," in *IEEE Antennas and Wireless Propagation Letters*, vol. 20, no. 3, pp. 411-415, March 2021.
- [27] G. H. Lee, S. Kumar, H. C. Choi and K. W. Kim, "Wideband High-Gain Double-Sided Dielectric Lens Integrated With a Dual-Bowtie Antenna," in *IEEE Antennas and Wireless Propagation Letters*, vol. 20, no. 3, pp. 293-297, March 2021.
- [28] S. Lei, K. Han, X. Li and G. Wei, "A Design of Broadband 3-D-Printed Circularly Polarized Spherical Luneburg Lens Antenna for X-Band," in *IEEE Antennas and Wireless Propagation Letters*, vol. 20, no. 4, pp. 528-532, April 2021.
- [29] R. Cicchetti, V. Cicchetti, A. Faraone, L. Foged and O. Testa, "A Compact High-Gain Wideband Lens Vivaldi Antenna for Wireless Communications and Through-the-Wall Imaging," in *IEEE Transactions on Antennas and Propagation*, vol. 69, no. 6, pp. 3177-3192, June 2021.